Presented at the Symposium on Optical Materials for High Power Lasers,
Boulder, Colorado, October 24-26, 1994
To be published in SPIE Proceedings,
Vol. 2428 (1995)

Reduction in Fiber Damage Thresholds Due to Static Fatigue

Robert E. Setchell

Sandia National Laboratories
Albuquerque, New Mexico 87185

ABSTRACT

For a number of years we have been investigating laser-induced damage mechanisms that can occur during the transmission of Q-switched, Nd/YAG laser pulses through fused silica fibers. We have found that fiber end-face characteristics, laser characteristics, and aspects of the laser-to-fiber injection typically determine dominant damage mechanisms. However, an additional damage process has been observed occasionally at internal sites where fibers were experiencing significant local stresses due to fixturing or to bends in the fiber path. A transmission reduction prior to damage was typically not measurable at these sites. Damage would not always occur during initial testing, but sometimes occurred later in time at laser levels that previously had been transmitted without damage. In these cases the time at stress appeared to be more important than the number of transmitted shots prior to damage. A possible relation between internal damage thresholds at stressed sites and the total time under stress is suggested by the fact that silica fibers experience static fatigue processes. These processes involve the slow growth of local defects under tensile stress at rates that depend upon environmental conditions. Defects reaching sufficient size and having appropriate location could be sites for reduced laser-induced damage thresholds. This possibility could have important implications for high-power fiber transmission systems that must satisfy extended lifetime requirements.

The needs of the telecommunications industry have motivated extensive studies into initial fiber defect characteristics and their likely growth mechanisms. The present work used the understanding developed in these studies to guide a preliminary experimental investigation into the possibility that static fatigue processes can affect damage thresholds. The experiments used a laser injection and fiber routing configuration that produced significantly elevated fluences within fiber core regions under tensile stress. In one set of experiments, internal damage thresholds were determined in available fiber samples that had been assembled in stress-imposing fixtures for periods up to 24 months. A decline in mean thresholds with time was observed, although measured values showed significant scatter. In order to establish initial strength and fatigue properties for these fibers, a number of additional samples were used to generate time-to-failure data at various stress levels. Based on these results, other fiber samples were subjected to conditions that greatly accelerated fatigue processes. Internal damage thresholds were then measured in these fibers and compared to thresholds measured in fresh fibers. Conclusive comparisons were frustrated by sample-to-sample and lot-to-lot variations in fiber defects.

1. INTRODUCTION

Various damage mechanisms that can limit the transmission of very high optical powers through fibers have been discussed previously.[1-4] Past studies primarily emphasized the effects of fiber end-face preparation, laser characteristics, and various aspects of laser injection into a fiber, since the damage mechanisms associated with these factors typically predominate in practice. If these mechanisms have been addressed with some success, however, the limiting damage process in a fiber transmission system may occur internally at sites that are typically under stress due to fixturing or to bends in the fiber path. Severe macrobends and microbends were carefully introduced in one study[4] to examine conditions that would immediately cause a stressed site to be the most likely to damage along the fiber path. These conditions resulted in measured reductions in fiber transmission, indicating that significant fluences were passing beyond the core/cladding interface due to the locally imposed changes in optical waveguide properties. Other studies found preferential internal damage at stressed sites that showed no measurable transmission reduction prior to damage.[1,2] Since total internal reflection appeared to be preserved at these sites, local focusing within the fiber core resulting from the imposed boundary conditions was a likely factor. Damage would not always occur at these sites during initial testing, but occasionally occurred later in time at an energy level that had been transmitted previously. The total time the fiber sample had been under stress appeared to be more important than the number of laser pulses prior to damage, although this distinction was not carefully addressed. The location of damage sites within the fiber cross section and possible correlations to imposed stresses were not examined in these early studies.

Past studies only speculated on the possibility that internal damage thresholds in a stressed fiber could depend on total time under stress in some manner related to static fatigue processes. Because some applications of interest may require extended fiber lifetimes, such a possibility could eventually affect the reliability of these fiber systems. The present study is an initial effort to seek evidence and to gain insights into this possibility. Fortunately, the expanding needs of the telecommunications industry have resulted in extensive studies of static fatigue processes in silica fiber.[5] Starting from the basis of fracture mechanics of brittle materials, initial fiber strength is related to the size distribution of flaws that inevitably result from fiber fabrication processes and from handling. These flaws are typically surface microcracks, although bulk defects are also present. Testing methods and standards have been established for characterizing fiber defect distributions. The reduction in fiber strength over time is described by models for the growth of flaws due to stress-enhanced chemical reactions that occur at crack tips. Water is the principal corrosion agent, with measured crack growth rates quite sensitive to humidity as well as temperature. Again, testing methods and standards have been developed to establish values for fatigue parameters given by common growth models. The current understanding of initial defect characteristics and fatigue mechanisms is sufficiently mature that engineering predictions based on standardized testing are routinely made for minimum fiber lifetimes in a variety of applications.

A high-power fiber system requiring a long lifetime obviously must be concerned with eventual catastrophic fiber failure due to fatigue processes. However, the ability to make conservative predictions based on some measure of necessary fiber testing is well established. The present study addresses the more subtle issue of whether damage thresholds can degrade in time in such a high-power system due to fatigue processes. For this possibility to have credibility, there must be an opportunity for defects to grow within fiber regions carrying significant laser fluences, and these defects must become preferential sites for laser-induced damage. Reductions in surface damage thresholds with increasing flaw sizes are well established in non-fiber applications,[6] with a general guideline being that defects having dimensions greater than one hundredth of the laser wavelength can adversely affect thresholds. As will be discussed shortly, fiber defects having such dimensions are likely to be found in standard production fibers. The likelihood of finding such defects within fiber regions carrying significant fluences can depend on the type of fiber. In our studies we have used multimode, step-index fibers having typical core and cladding diameters of 400 and 440 microns, respectively. Near-field profiles of laser fluences at the exit faces of these fibers show a sharp cutoff at the core/cladding interface (any light injected into the cladding is quickly lost at the cladding/buffer interface). Calculations of the penetration of evanescent fields into the cladding show that these fields extend over dimensions that are small compared to the cladding thickness (less than a micron for most fiber modes). Consequently, it appears unlikely that defects external to the core/cladding interface can affect damage thresholds. One common type of step-index fiber has a hard polymeric cladding added to a pure silica core drawn from a homogeneous silica preform. Typical surface microcracks are expected to be found penetrating into the fiber core at the core/cladding interface. Fatigue studies on such fibers have shown high initial strengths (small initial defects), but atmospheric water penetration through the polymeric cladding still results in defect growth under tensile stress.[7] Consequently, this type of fiber appears to be a good candidate for defect growth in fiber regions experiencing significant laser fluences. Most of our studies have used another type of fiber having a fluorine-doped, fused silica cladding surrounding a pure silica core. These fibers are drawn from preforms having the same core/cladding structure, and surface microcracks are to be expected at the cladding/buffer interface. However, the preforms used for drawing this fiber were originally homogeneous rods of pure silica. The fluorine-doped silica cladding layer is added to these rods through a chemical plasma deposition process.[8] The resulting core/cladding interface could still have surface flaws associated with the original silica/air interface, modified in some way by the plasma deposition process. An obvious path for atmospheric water to reach defects at the core/cladding interface is lacking, however. Whether or not the high concentration of hydroxyl radicals (600-800 ppm) in the core of "high OH^-" silica fiber (which we have typically used) can be a factor for internal defect growth is not known. Although this type of fiber appears to be a less likely candidate for defect growth in fiber regions experiencing significant laser fluences, the preliminary experiments in the present study used only this fiber type.

In a previous study, linear arrays of fibers were assembled into machined fixtures designed to impose predictable stresses along the fiber path.[3] These fibers were tested for damage thresholds using a fiber-to-fiber injection method that eliminated effects of laser mode structure and minimized peak fluences throughout the fiber path. Some of these fibers did not damage during the testing procedure, and the rest only damaged at the fiber entrance face. A few assemblies were taken apart after testing, but the rest were kept intact and stored in ambient conditions. As a convenient means of testing fibers subjected to known tensile stresses for some period of time, these fiber assemblies were tested again following careful repolishing of the entrance faces. A simple fiber injection method using a 50-mm focal length lens[4] was used for this retesting rather than the

more complex fiber-to-fiber injection method. With this simple method a few fibers had been examined after storage periods of one and 18 months, and the remainder were examined in this study after a storage period of 24 months.

The retesting of fixtured fibers motivated interest in the initial strength and fatigue characteristics of these particular fibers. Using fiber samples of the same type from the same manufacturer (but from a different production lot), time-to-failure testing was conducted by wrapping samples around different diameter mandrels. Based on initial tests that gave consistent results for fatigue behavior, a particular stress level and time-at-stress were selected for subjecting two-thirds of a recent batch of polished fiber samples (same manufacturer and type but another production lot) to "accelerated aging" conditions. These conditions were intended to produce defect growth for a time that would represent a large fraction of the expected time to failure. Unfortunately, the accelerated aging condition resulted in the immediate failure of many of the polished fibers. Fibers that survived the aging process were damage tested using the simple lens injection method, and the results were compared to thresholds obtained by damage testing the third of the recent batch of polished fibers that did not experience the aging process.

Following a brief section summarizing initial strength and fatigue characteristics, the experimental configuration used in the present study will be described. This configuration subjected the initial length of a test fiber under stress to elevated laser fluences in the portion of the fiber cross section under tensile stress. When subjecting fibers to accelerated aging conditions, the fiber samples were carefully marked to indicate the side of the fiber that had experienced the peak tensile stresses. When these fibers were subsequently mounted for damage testing, the same fiber side was positioned to experience peak tensile stresses and elevated fluences. This method of fiber indexing allowed us to examine damaged fibers for correlations between damage sites and the cross-sectional regions that had experienced high stresses and elevated fluences. Subsequent sections present and discuss the various experimental results.

2. STATIC FATIGUE PROCESSES

The information that follows is simply intended to be a synopsis of general understanding of fiber defect and fatigue characteristics.[5] Although the theoretical strength of fibers made from pure fused silica is extremely high, in practice the strength of any fiber will be limited by unavoidable defects. A freshly drawn silica fiber will have some distribution of surface (microcrack) and bulk defects, as indicated in an exaggerated manner by the sketch in Fig. 1. The expanded view of a small section of the surface shows a surface microcrack, with "a" representing the crack length. If this section of fiber is subjected to a tensile stress σ, the stress at the crack tip is intensified. A stress intensity factor, K_I, is defined by:

$$K_I = Y\sigma\sqrt{a} \tag{1}$$

where Y is a constant that depends on the crack geometry. If the applied stress is increased continuously, complete fracture of the fiber cross section will occur at a critical value of the stress intensity factor, K_{Ic}, which depends only on material properties. For a sample of fiber in which "a_0" represents the maximum depth of all surface microcracks, failure of this section will occur when the applied stress reaches a value given by:

$$S_0 = \frac{K_{Ic}}{Y\sqrt{a_0}} \tag{2}$$

Equation (2) identifies the initial strength, S_0, of this fiber sample. Figure 2 shows this relation plotted for fused silica using a representative value for Y. During the fiber drawing process, manufacturers will conduct an on-line proof test in which the freshly drawn fiber is subjected to a given tensile stress for a short period of time (≈1 s). Any sections of fiber that fail are eliminated from the final batch. The stress applied during the proof test effectively eliminates all defects in the fiber batch above a size given by Eqn. (2). For example, a typical proof test level of 100 kpsi ensures that the fiber will not have defects larger than ≈0.7 micron. Consequently, typical proof test values only ensure that the maximum size of fiber defects is comparable to laser wavelengths. In fact, if fibers are manufactured using the highest quality preforms and if drawing processes are carefully controlled, the actual size distribution of defects can be much smaller. Some manufacturers have the capability for generating failure statistics that give accurate descriptions of actual defect distributions. The necessary testing may involve loading fiber samples of a given length at a selected strain rate until they fail at some stress level that is

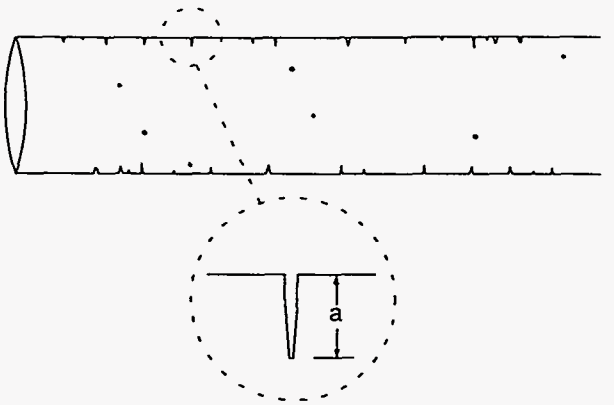

Figure 1. Defects in freshly drawn silica fibers

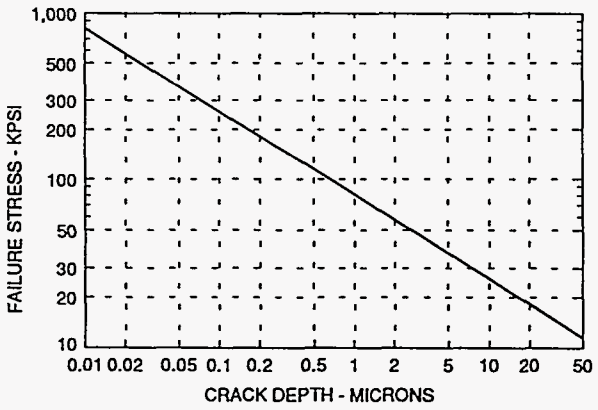

Figure 2. Failure stress versus microcrack size

recorded. A large number of samples are required for accurate statistics, and the particular sample length used and the strain rate chosen can affect the results. Such results are typically plotted in terms of failure probability versus breaking stress (Weibull plots), and will have regions with different slopes that distinguish very small intrinsic defects from defects that were introduced during manufacturing or in subsequent handling. In the absence of such detailed information, the fiber user can only be assured that his samples have defects no larger than the size established by the manufacturer's proof test.

Fiber fatigue (or "corrosion") involves the slow growth of defects within fiber sections under tensile stress at rates that are dependent upon environmental conditions. This progressive reduction in fiber strength results in a finite lifetime for any silica fiber under static tensile stress. In any practical application, fixturing and routing requirements will ensure that some sections of fiber will be under tensile stress. Models relating the rate of crack growth to the applied tensile stress often assume a power-law form:

$$\frac{da}{dt} = A(K_I)^n \tag{3}$$

where the crack dimension "a" and the stress intensity factor K_I have been introduced previously. The parameters A and n are dependent on environmental conditions, with the exponent n typically called the static fatigue parameter (or corrosion susceptibility). Investigations into the chemical mechanisms for crack growth in silica indicate that this power-law form is only approximate, and a more fundamental relation between crack velocity and applied stress has an exponential form.[9] For present purposes the simple power-law form of Eqn. (3) will be used. Substituting for K_I using Eqn. (1), Eqn. (3) can be integrated to give crack dimensions as a function of time for a given stress history $\sigma(t)$. Predicted failure times can be derived from this expression, with the integration most conveniently performed in terms of the time-varying fiber strength:

$$S(t) = \frac{K_{Ic}}{Y\sqrt{a(t)}} \tag{4}$$

For a static stress σ = constant, integration of Eqns. (3) and (4) predicts failure at a time given by:

$$t_f = B S_0^{n-2} \sigma^{-n}, \quad \text{where} \quad B = \frac{2K_{Ic}^{2-n}}{(n-2)AY^2} \tag{5}$$

S_0 is the initial fiber strength given by Eqn. (2). The result in Eqn. (5) assumes $\sigma << S_0$ and $n >> 1$, as are typically true in practice. Equation (5) can be used to predict fiber lifetimes if the peak tensile stress, the initial fiber strength, and the fiber fatigue parameters are known. A common approach to determining fatigue behavior is to use the fact that Eqn. (5) can be written:

$$\log(t_f) = n\log(\sigma_1) - n\log\sigma \tag{6}$$

where failure time t_f is expressed in seconds, and σ_1 is the static stress level that results in a failure time of 1 second. Test techniques have been developed for making measurements of failure time versus static stress over a sufficient range in stress values for the parameters n and σ_1 to be determined. Figure 3 shows a few examples of such tests conducted on silica fibers with hard polymeric coatings.[10] All samples were stored in the intended test condition for five days prior to the application of tensile stresses. The curves are linear fits (in a log-log plane) to numerous data points obtained by applying different static stresses over a range of 350-750 kpsi, with corresponding failure times from 10^3 to 10^7 seconds. A large number of 1.0 meter samples were used to generate these curves, and the actual data over the tested stress range show little scatter from the linear fits. The results in Fig. 3 show exceptionally high 1-second strengths compared to typical proof test levels, indicating that the initial defect sizes were much smaller than would have been detected by a proof test. This strength is degraded by presoaking the fibers in water, and the fatigue parameter n is reduced (reducing the time-to-failure for a given stress) by increasing temperature and relative humidity.

It is useful to examine the actual growth of a microcrack over time until the time predicted for fiber failure. By directly integrating Eqn. (3) for a static stress σ, then using Eqn. (5), we find:

$$\frac{a(t)}{a_0} = (1 - t/t_f)^{\frac{-2}{n-2}} \tag{7}$$

This expression describes crack growth behavior over the course of the expected fiber lifetime as a function of the fatigue parameter n. As discussed previously, the lifetime t_f is itself a sensitive function of the value of n. Figure 4 shows the crack behavior for a range of values for n. Only when the value of this parameter is relatively small (n < 10) is there significant change in crack dimensions throughout the fiber lifetime. For larger values of n there is little observable growth until the failure time is approached. Fatigue testing results[7,10] find values of n to be at least 15 under the harshest environments, and typically from 20 to 30 under more benign environments. Consequently, Eqn. (7) indicates that microcrack dimensions grow very slowly over most of the expected lifetime, with significant changes only occurring close to the expected time for catastrophic fiber failure. This equation is based on an assumed power-law relation between crack velocity and the stress intensity factor (Eqn. (3)). If crack velocity has an exponential dependence on stress intensity, however, crack growth as a function of time over the expected fiber lifetime will have different behavior. Practical measurements of crack velocity in silica under stress are made over a limited range of stress intensity values, and within this range there may not be significant differences between power-law and exponential fits. If both fits are made to such data, however, the resulting exponential expression predicts crack velocities many orders of magnitude greater than the power law fit at stress intensities lower than the experimental range.[9] This would have the effect of accelerating the initial crack growth and reducing the overall time to failure. Therefore, the curves in Fig. 4 may show smaller increases in crack dimensions over much of the fiber lifetime than actual crack behavior. Equivalent calculations assuming an exponential dependence would be very useful for comparisons, but this dependence does not lead to simple analytical expressions like Eqns. (5) and (7).

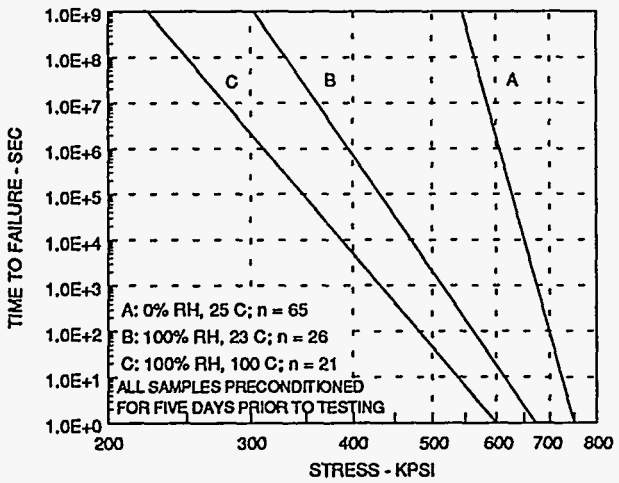

Figure 3. Fatigue testing of silica fibers with hard polymeric coatings (Ref. 10)

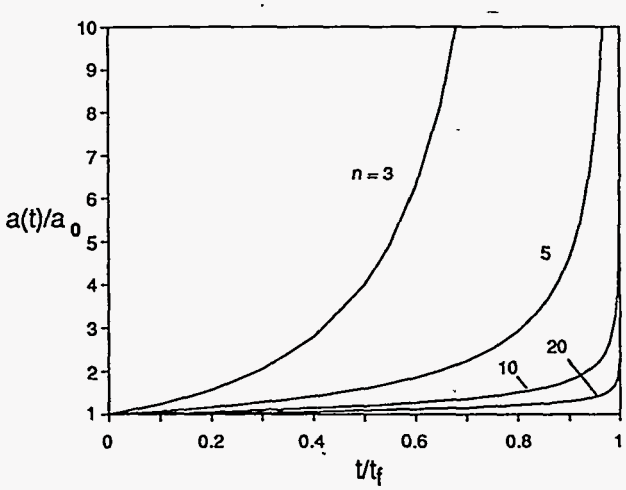

Figure 4. Crack growth as a function of the fatigue parameter n

3. EXPERIMENTAL CONFIGURATION

The basic experimental configuration using a simple lens (50 mm focal length) for laser injection was described previously.[4] The test laser operates at a wavelength of 1.06 micron and has a pulsewidth of 11.5 ns. Testing procedures and damage diagnostics were essentially the same as in past studies. The position of the entrance face of test fibers beyond the focal plane of the laser focusing lens was increased slightly to reduce the ratio of peak incident fluence to "average core fluence" (defined as the incident pulse energy divided by the fiber core area) to a nominal value of 3.5. All fibers tested in the current study had a 400-micron diameter core of high-OH^- fused silica, a 20-micron thick cladding of F-doped fused silica (resulting in a numerical aperture of 0.22), and a 15-micron thick polyimide buffer. Carefully machined plastic fixtures were used to control the path of test fibers throughout most of their length. The nominal fixture introduces a 15.2-cm diameter loop within the overall fiber length of 82 cm. A straight entrance path (≈18 cm long) precedes the constant-diameter path within the loop, and a straight exit segment completes the path. The axis of the entrance path is always carefully aligned with the laser axis to avoid "entry" damage.[4] Machined fixtures having smaller loop diameters have also been used to impose higher tensile stresses on test fibers, and a few were used in the present study. Each test fiber was aligned using a very low laser energy, then subjected to a series of single laser pulses in which the energy was increased with each successive pulse. In the current studies, a total of 15 pulses were used to reach a maximum transmitted energy of 110 mJ. Damage was typically detected well before the maximum energy was attained, and entrance-face breakdown[4] often occurred prior to permanent damage.

Choosing a focal length of 50 mm for the injection lens was based on air breakdown thresholds for our laser. A shorter focal length would have been desirable in terms of filling more of the available fiber modes (a focal length less than ≈15 mm would be necessary to make full use of the numerical aperture). For focal lengths less than 50 mm, however, air breakdown can occur prior to reaching the maximum test energy. In previous studies we did not carefully consider if this "low-angle" injection method would result in seriously elevated fluences at internal locations within the fiber. Details of the injection geometry can certainly affect "entry" damage, but careful alignment typically mitigates this problem to where other damage mechanisms dominate. Entrance-face and exit-face damage, for example, are clearly based on other factors. Nevertheless, elevated internal fluences could result from focusing effects within an initial portion of the fiber path before sufficient bends in the path promote random mixing into higher modes. Results obtained during the current study prompted us to investigate this possibility in more detail. Information generated by this investigation is relevant for interpreting the results of current experiments on possible effects of fatigue processes, and a summary of this information will be presented first.

Figures 5 and 6 identify a likely mechanism for generating high laser fluences within the portion of the fiber path where a transition is made from a straight entry segment to a segment at a constant bend radius. Figure 5 shows a meridional ray within the plane of the figure that initially makes an angle θ with respect to the fiber axis. If this angle is sufficiently small, the ray will only reflect from the outer core/cladding interface within the bend. Borrowing a term from acoustics, such a ray is known as a "whispering gallery" ray.[11] The range of angles resulting in such rays depends on the fiber radius, the bend radius, and the position of the ray as it enters the bend. For the case of a 400-micron diameter fiber entering a bend having a constant radius of 7.6 cm, rays passing through the fiber axis at the bend entrance will become whispering gallery rays if their angle θ is less than $\approx 4°$. For large step-index fibers that can support many thousands of modes, the distribution of optical power within these modes can be expressed as a continuous function of the angle each mode makes with the fiber axis.[12] The initial mode power distribution (MPD) generated in our test fibers using our laser and our lens injection method is shown in Fig. 6. Essentially all of the laser energy is confined within angles less than 2°, which is far less than the maximum angle of 8.7° for total internal reflection in this case.

These figures suggest that laser fluences can be concentrated near the outer portion of the fiber cross section after entering the bend introduced by our test fixtures, and this concentration is enhanced by our "low-angle" injection geometry. To confirm that this actually occurs in our experiments, fibers were potted into several 15.2-cm diameter fixtures using a low-shrinkage epoxy in order to permanently fix their path consistent with typical testing conditions. Each fixture was then sawed in two at a different angular position in the bend past the transition plane (dotted line in Fig. 5). The sectioned fixtures were carefully polished where they had been cut, then positioned with respect to the injection optics in the same manner as an intact fixture with a fresh test fiber. A magnified beam-profiling system was then used to obtain near-field profiles at the fiber exit faces.[3] Figure 7 shows a profile obtained at an angle of 43° past the transition plane. The "outside" of the fiber (farthest from the center of curvature) is on the left side in this figure. If "average" fluence is defined as the total pulse energy divided by the

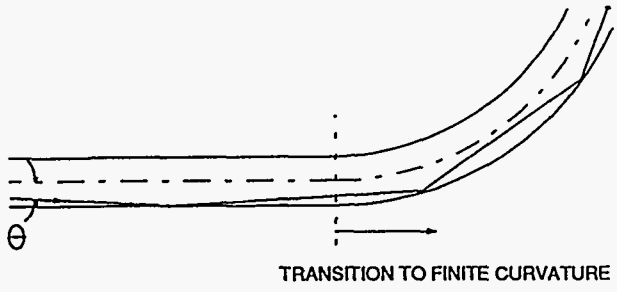

Figure 5. "Whispering gallery" rays

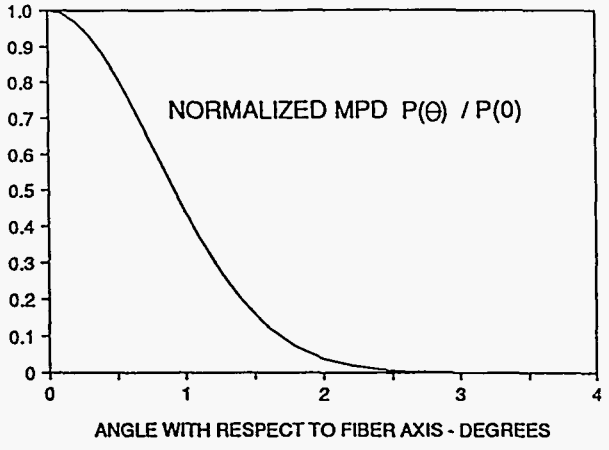

Figure 6. Initial mode power distribution (MPD)

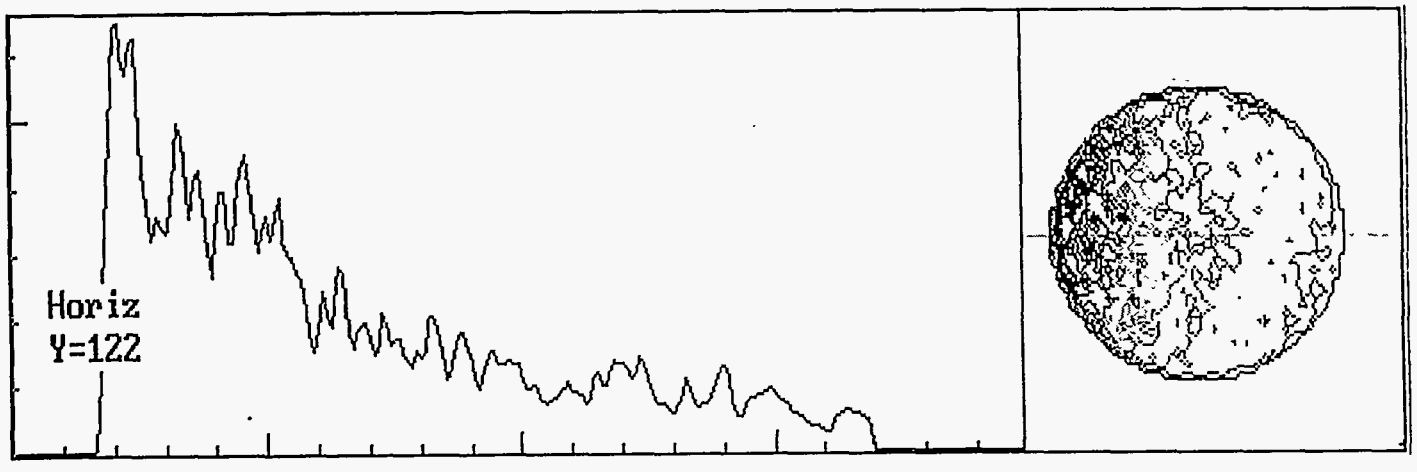

Figure 7. Fiber near-field profile at a position 43° beyond the start of a bend having a constant 7.5-cm radius

fiber core area, then the profile shown in Fig. 7 has a peak fluence that is 5.0 times higher than the average. This peak fluence is substantially higher than the peak fluence incident on the fiber entrance face (for a given pulse energy). Defects near the "outside" core/cladding interface obviously would be more likely to precipitate damage than defects elsewhere within the fiber core. The profile shown in Fig. 7 is very sensitive to the alignment of the initial (straight) portion of the fiber with respect to the laser axis. When this alignment was intentionally offset up to ±100 microns along both horizontal and vertical axes, the ratio of peak to average fluences varied from 4.2 to 9.6. A profile similar to that shown in Fig. 7 was also observed at an angle of 23° beyond the transition plane. At this position the ratio of peak to average fluences was found to be 4.1.

These observations confirmed that our experimental configuration results in locally high fluences within the fiber core after the transition to a constant-diameter loop, and that the peak fluences occur near the core/cladding interface farthest from the center of curvature. The same region of the fiber core is under tensile stress due to the imposed curvature. If defects are present near the core/cladding interface in this region, this experimental configuration provides a severe test for their susceptibilty to damage.

4. RETESTING OF STORED FIXTURES

In experiments performed in 1992, linear arrays of fibers were assembled into machined plastic fixtures and tested using a fiber-to-fiber injection system.[3] These experiments examined the effects of different entrance-face preparation steps, and also subjected fibers to static stress levels of 30, 60, and 90 kpsi using fixtures with 360° loops having diameters of 15.2, 7.6, and

5.1 cm, respectively. The fiber-to-fiber injection system produced relatively low peak fluences on the entrance face of test fibers (a peak-to-average fluence ratio of 3.3) and an injection geometry that used far more of the available fiber numerical aperture than a simple lens approach. A surprising number of the test fibers did not damage within our testing range (demonstrating the value of a particular conditioning schedule using a CO_2 laser), and the remainder only experienced entrance-face damage. After these experiments were concluded, a few assemblies were taken apart and their undamaged fibers used for other purposes, but the rest were simply stored under ambient conditions. In the present study these stored assemblies were retested as a convenient means of examining fibers subjected to known static stress conditions for an extended period of time. Rather than assembling the rather complex fiber-to-fiber injection system again, we utilized the simple lens injection method that had been used in more recent studies. One obvious difficulty was the need to repolish the entrance faces of the fibers that had damaged in the 1992 experiments. Special fixtures were designed and fabricated that held the complete assemblies (typically containing 10 fibers) in such a manner that all of the entrance faces in an array could be hand polished simultaneously. With one exception, a mechanical polishing schedule similar to the baseline schedule reported in previous studies was used. The exception was to add a final polishing step using a commercial colloidal silica suspension.[13]

The results of the retesting experiments are shown in Figs. 8 and 9. Figure 8 shows the original testing results obtained in 1992. The two curves give the percent of tested fibers that transmitted a given energy before either entrance-face breakdown or permanent damage (entrance face only) occurred. Only shown in this figure are results obtained with fibers having a baseline mechanical polish. Not shown are results with fibers that had been CO_2-laser polished. One laser polishing schedule resulted in fibers that showed minimal entrance-face breakdown and no permanent damage over this testing range. Figure 9 shows the results of the recent retesting of these fibers. Every retested fiber damaged, making it possible to present the results in terms of the mean value and standard deviation of the maximum energy transmitted before damage. In addition to results obtained after 24 months of storage, Fig. 9 shows some measurements made at earlier times. These consist of a few undamaged fibers from the 1992 study that were removed from their fixtures after one month, and a few undamaged, fixtured fibers that were retested after 18 months. The numbers by the data points indicate how many fibers were tested, and sufficient samples to generate accurate statistics were only used after 24 months. Every retested fiber damaged early in the first quadrant of the constant-diameter loop following the straight initial fiber segment. No significant differences were noted in damage levels between fibers in 15.2-cm and 7.6-cm diameter fixtures, and these results are combined in Fig. 9. The "zero time" data shown in this figure are results obtained with cleaved fibers that were tested with a 15.2-cm diameter fixture and the same lens injection system in a previous study.[4] A few measurements resulting in very early damage at clearly contaminated surfaces have been eliminated from the "zero time" data. Only one-third of these fibers damaged in the same internal region as the retested fibers. The fibers retested after 24 months of storage had been repolished using a colloidal silica suspension as the final polishing step. Significantly, none of these fibers experienced entrance-face breakdown prior to permanent damage.

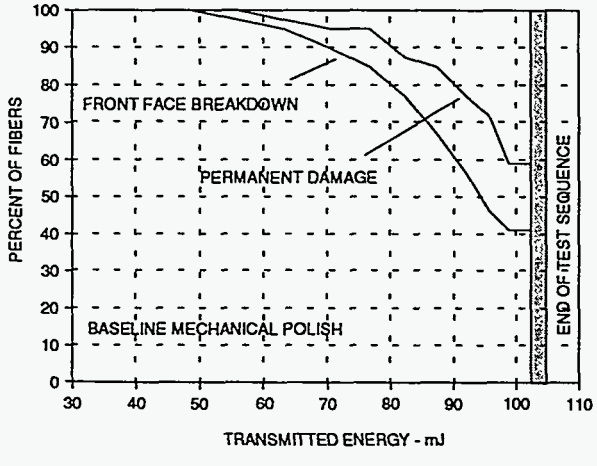

Figure 8. Previous damage testing results

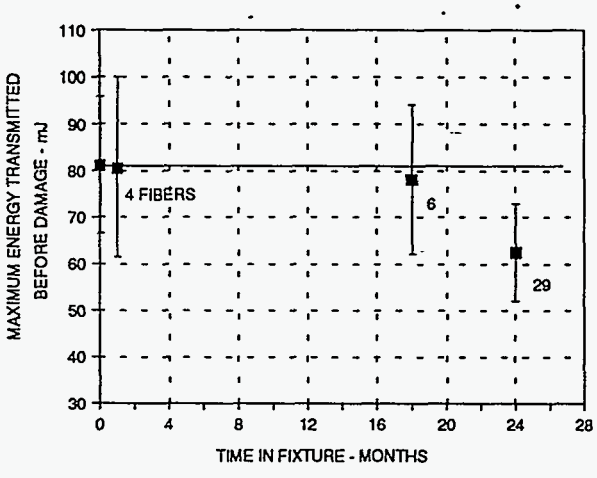

Figure 9. Results of retesting 1992 fiber assemblies

5. ACCELERATED AGING STUDY

The measurements on retested fibers (Fig. 9) suggest that internal damage thresholds in the initial bend region may have started to fall by 24 months. A more definitive conclusion is hindered by the large standard deviations and the lack of good

statistics under identical testing conditions before and after storage. In addition, there were no significant differences between thresholds measured in fixtures having diameters of 15.2 and 7.6 cm, even though the corresponding peak static stresses varied by a factor of two. Nevertheless, the fact that there may have been a reduction prompted us to investigate the initial strength and fatigue characteristics of these fibers. Although none of the particular fiber production lot used for the 1992 assemblies was still available, we had on hand a new batch of 60 polished (baseline mechanical schedule) fiber samples from a different production lot of the same fiber type and manufacturer. In addition, we had a substantial quantity of bulk fiber from yet another lot of the same fiber type and manufacturer. This bulk fiber was used to examine the initial strength and fatigue characteristics of this fiber type. Our goal was to establish these properties with sufficient accuracy that conditions could then be identified for quickly "aging" some fraction of the new polished fibers to promote internal defect growth. Damage thresholds obtained on "aged" fibers could then be compared with thresholds obtained on new fibers that did not experience the accelerated aging conditions.

Initial strength and fatigue properties were examined by conducting time-to-failure tests at several static stress levels obtained by wrapping fiber samples around polished mandrels having different diameters.[7] Uncontrolled ambient laboratory conditions were chosen for simplicity (this had been the storage environment for the retested 1992 fibers). Failure times less than a few hours were detected by direct observation. For longer failure times, a thin (40 gauge) transformer wire was taped across the coils of fiber wrapped on each mandrel. Each wire completed a circuit powering a digital time-totaling clock. When a highly stressed fiber would fail, the violent motion of the fractured ends would cut the transformer wire and stop the corresponding clock. After approximately 30 fiber samples were used to measure failure times at stress levels between 440 and 555 kpsi, the power-law fatigue curve shown in Fig. 10 was indicated. This curve has a 1-second strength of 640 kpsi and a fatigue parameter of n≈34. This initial strength is very high compared to typical proof test levels, but not as high as the dry fiber strength shown in Fig. 3. The fatigue parameter is consistent with the range that might be expected (≥30) for polyimide-buffered silica fibers under relatively dry conditions.[14] These values for initial strength and fatigue parameter would predict that initial defect sizes in our retested fibers (Fig. 9) would be very small (<0.02 μm), and that defect growth within 24 months would be negligible. Based on this indicated behavior, an accelerated aging condition consisting of a stress of 415 kpsi for $6x10^5$ seconds (7 days) was selected. As shown in Fig. 10, this condition would subject the fibers to a significant fraction of the lifetime at this stress (≈35 days) that would be expected if this assumed fatigue behavior was accurate. A number of polished mandrels having the proper diameter to produce a peak tensile stress of 415 kpsi were then prepared.

When a polished fiber sample was wrapped on one of the 415 kpsi mandrels, the exterior side of the fiber was marked to permanently index which side had experienced peak tensile stresses. This indexing is indicated in the sketch shown in Fig 11. When these fibers were subsequently mounted in standard test fixtures, the same fiber side was positioned to the outside of the loop in order to again be subjected to tensile stresses. As discussed in the section on the current experimental configuration,

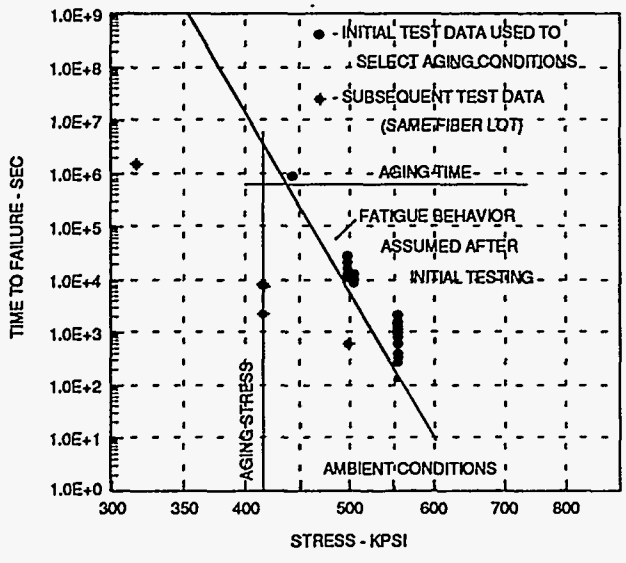

Figure 10. Initial strength and fatigue behavior testing

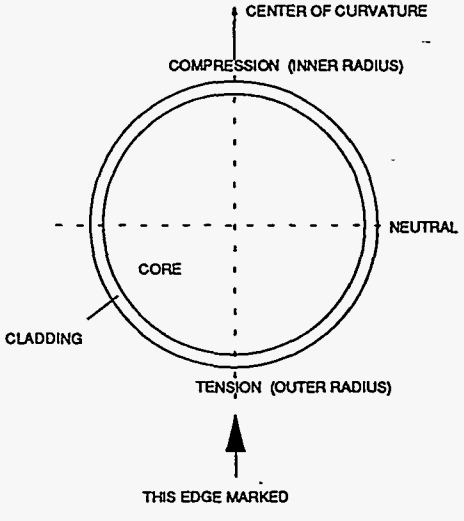

Figure 11. Indexing of fibers subjected to accelerated aging

this positioning caused the "aged" side of the fibers to be subjected to significantly elevated fluences. Unfortunately, half of the polished fibers did not survive the accelerated aging condition. A total of 38 polished fibers were used to finally produce 18 "aged" samples suitable for damage testing. A third of the fibers that failed either broke during mandrel wrapping or failed within a few minutes. This unexpected result caused us to return to time-to-failure testing at this stress level and others using the remainder of our bulk fiber lot. The additional data points shown in Fig. 10 were eventually obtained, indicating that the fatigue behavior initially assumed for this fiber was quite optimistic. In addition, fiber samples from another bulk lot on hand were subjected to the 415 kpsi stress and found to fail at times that ranged from immediate (during wrapping) to 9 days. Clearly, these additional time-to-failure tests were revealing fiber samples having much lower initial strength (larger initial defects) than the samples initially used to establish the accelerated aging condition. This difference could be due to lot-to-lot variations and to sample-to-sample variations that require far more time-to-failure tests than we had conducted in order to achieve an accurate characterization. Furthermore, additional defects that reduce initial strength could have been introduced to our polished fibers during the handling-intensive polishing processes.

The fibers that did survive the accelerated aging condition were loaded into standard test fixtures and damage tested. For comparison, the polished fibers that had not been "aged" were similarly tested. Curves showing the percent of test fibers that transmitted a given energy before permanent damage are plotted in Fig. 12. Most of these fibers experienced entrance-face breakdown prior to permanent damage, but for simplicity these curves are not shown. For fibers not subjected to the accelerated aging condition, the maximum energy transmitted before damage had a mean value of 71 mJ and a standard deviation of 17 mJ. Seventeen of these fibers were tested, and 13 damaged early within the first quadrant of the constant-diameter loop following the straight initial segment. Five of these fibers damaged simultaneously at two or three separate sites within the first quadrant of the loop. For fibers that had survived the accelerated aging condition, the maximum energy transmitted before damage also had a mean value of 71 mJ but a standard deviation of only 11 mJ. Damage within the first quadrant of the fixture loop occurred in 14 out of 18 of these fibers. Seven of these fibers damaged simultaneously at up to five separate sites spaced throughout the first loop quadrant. Because these fibers had been indexed prior to testing, damage sites were examined with a microscope to establish correlations between these sites and the region within the fiber core that had experienced both aging stresses and elevated fluences. An example is shown in Fig. 13. The orientation of this photo is the same as the sketch shown in Fig. 11. A very smooth cleaving was produced over much of the fiber core by the damage that originated near the core/cladding interface. The damage sites in every aged fiber appeared to have the same location as the example in Fig. 13.

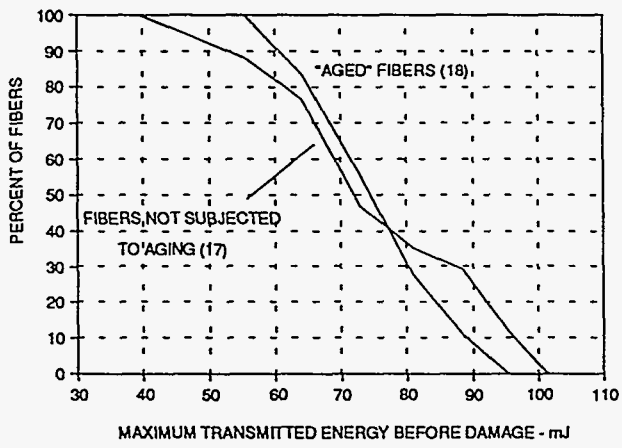

Figure 12. Comparative thresholds in "aged" fibers

Figure 13. Damage in an "aged" fiber

6. DISCUSSION

A high-power fiber system requiring a long lifetime obviously must be concerned with static fatigue processes that can eventually cause catastrophic fiber failure, but the means to assess and manage this concern are well established. A possible

relation between static fatigue processes and fiber damage thresholds is far more speculative, but the potential consequences are of sufficient concern to motivate careful investigation. The current study is a preliminary attempt to seek evidence and to gain insights into this possibility. We have found that certain challenges must be faced in making such an attempt. The first challenge is the basic question of whether there is a valid mechanism for stress-driven growth of defects near the core/cladding region in fibers having F-doped silica claddings, as have been used in our studies. A second challenge is the fact that current models for microcrack growth predict very slow defect enlargement over most of the expected fiber lifetime. A final challenge is the fact that defect distributions in fiber samples depend on preform characteristics, drawing processes and controls, coating processes and controls, and subsequent handling. Significant lot-to-lot and sample-to-sample variations may be inevitable. Without experimental observations to indicate otherwise, the first two challenges would suggest that significant fatigue effects on damage thresholds are unlikely. First of all there must be a reasonable mechanism for defect growth. For fibers with hard polymeric claddings, a mechanism based on atmospheric moisture for stress-driven growth of defects near the core/cladding interface appears to be well established. Whether a different growth mechanism is possible for our high-OH^- fibers with F-doped silica cladding is not known, and is beyond the scope of the present study. Even if such a mechanism exists, it may be masked in typical fatigue testing by the expected growth of surface microcracks. Secondly, there must be significant defect growth on time scales of interest. Assuming a power-law dependence between crack velocity and stress, the calculations in Fig. 4 indicate that the effects of microcrack growth can be neglected provided fiber use is kept well short of predicted times to failure.

With these challenges in mind, motivation for pursuing a relation between fatigue processes and damage thresholds must be based primarily on any laboratory experiences that suggest our understanding may be incomplete. As mentioned earlier, previous studies resulted in occasional observations that suggested internal damage thresholds may have a time-at-stress dependence. In the current study, the results from retesting fibers stored in stress-imposing fixtures (Fig. 9) indicated a possible threshold reduction after 24 months. Insufficient data points, large standard deviations, and changes in the testing configuration from that used in 1992 all contribute to minimizing the significance of this indication. In particular, the current experimental configuration imposed severely elevated fluences in the fiber regions where damage consistently occurred. Although this may be useful in terms of detecting defects that can precipitate damage near the core/cladding interface in fiber regions under tensile stress, direct comparisons with 1992 thresholds are negated. Interestingly, the need to repolish these fiber assemblies appears to have identified a polishing procedure (using colloidal silica) that increases the breakdown resistance of entrance faces. A possible non-fatigue explanation for the current retesting results and the previous observations could be based on the fact that our observations have all been with fibers that experienced at least a few high-fluence laser pulses prior to damage. Studies of cumulative effects on bulk damage thresholds in fused silica[15] have indicated that microscopic laser-induced changes can accumulate prior to macroscopic damage. However, these studies found that a large number of pulses (>1000) may be necessary to clearly establish a reduction of only ≈20% from single-pulse thresholds at a wavelength of 1.06 microns.

A satisfying approach to future studies would be to devise and conduct additional experiments in which possible effects of fatigue processes on internal damage thresholds over extended times could be identified unambiguously. Some method of accelerated aging seems necessary, although this will require consideration of the third challenge identified above. The time-to-failure measurements shown in Fig. 10 indicate that numerous samples from a particular lot are required to establish initial strength and fatigue characteristics for that lot. We also found significant lot-to-lot variations. Because of these factors, the accelerated aging condition used in the current study was more likely a means to select fibers with smaller initial defects (an extreme proof test) than a means to produce test fibers with enhanced defect growth. This possibility is supported by the fact that the smaller standard deviation found for the "aged" fiber threshold primarily corresponds to fewer fibers damaging at lower energies (Fig. 12). The location of damage sites in "aged" fibers correlated to the side of the fiber exposed both to high peak stresses during aging and to high fluences during testing (Figs. 11 and 13). The fact that every fiber damaged at or very near the core/cladding interface is strong evidence that defects distinct from bulk silica flaws are distributed at this interface. Even if local fluences were ten times higher than average fluences within the test fibers, all damage would have occurred at levels that are still considerably smaller than bulk silica thresholds expected for the same laser characteristics.[15] In future studies aimed at achieving unambiguous results, a single production lot of fiber should be used both for carefully establishing initial strength and fatigue characteristics, and for threshold testing before and after accelerated defect growth. Fiber samples for damage testing will need to be polished very carefully to prevent additional defects from being introduced. An experimental configuration that subjects "aged" regions of the core/cladding interface to elevated fluences (as in the present study) could be very useful for ensuring that damage would preferentially occur in this region rather than in other parts of the

fiber system. However, alignment sensitivity would have to be examined to make sure that consistent peak fluences would be achieved in every test fiber.

7. ACKNOWLEDGEMENTS

This work was supported by the U. S. Department of Energy under Contract DE-AC04-94AL85000. The author would like to thank Paul Klingsporn of Allied-Signal, Inc., Kansas City Division, for providing the polished fiber samples used in this study. The talented assistance of Dante Berry, Geo-Centers, Inc., Albuquerque, in repolishing the 1992 fiber assemblies, preparing and conducting the time-to-failure testing, and performing much of the damage testing, was greatly appreciated.

8. REFERENCES

1. R. E. Setchell, K. D. Meeks, W. M. Trott, P. Klingsporn, and D. M. Berry, "High-Power Transmission Through Step-Index, Multimode Fibers," Proc. SPIE 1441, 61 (1991).

2. R. E. Setchell and P. Klingsporn, "Laser-Induced Damage Studies on Step-Index, Multimode Fibers," Proc. SPIE 1624, 56 (1992).

3. R. E. Setchell, "Laser-Induced Damage in Step-Index, Multimode Fibers," Proc. SPIE 1848, 15 (1993).

4. R. E. Setchell, "Damage Studies in High-Power Fiber Transmission Systems," Proc. SPIE 2114, 87 (1994).

5. The literature is quite extensive in this area. For useful overviews, see: D. E. Quinn, "Optical Fibers," and M. M. Ramsay, "Fiber-Optic Cables," in Fiber Optics Handbook, F. C. Allard, Ed., McGraw-Hill, New York, 1990, pp. 1.39-1.45, 2.5-2.10.

6. R. M. Wood, Laser Damage in Optical Materials, Adam Hilger, Bristol, 1986, pp. 5-7; also: references cited within.

7. J. P. Clarkin, B. J. Skutnik, and B. D. Munsey, "Enhanced Strength and Fatigue Resistance of Silica Fibers with Hard Polymeric Coatings," J. Non-Crystalline Solids 102, 106 (1988).

8. "Fluosil® Fiber Optic Preforms," Heraeus Bulletin PLW-B1, Heraeus Amersil Inc., Duluth, Georgia.

9. T. A. Michalske, W. L. Smith, and B. C. Bunker, "Fatigue Mechanisms in High-Strength Silica-Glass Fibers," J. Am. Ceram. Soc. 74, 1993 (1991).

10. B. J. Skutnik, M. H. Hodge, and D. K. Nath, "High Strength, Reliable, Hard Clad Silica (HCS)™ Fibers," in: FOC/LAN 85 Proceedings, 1985, p. 232.

11. A. W. Snyder and J. D. Love, Optical Waveguide Theory, Chapman and Hall, London, 1983, pp. 180-188.

12. D. Gloge, "Optical Power Flow in Multimode Fibers," Bell Syst. Tech. J. 51, 1767 (1972).

13. Mastermet® Colloidal Silica Suspension used on TEXMET® cloth, both from Buehler, Lake Bluff, Illinois.

14. D. Roberts, E. Cuellar, and L. Middleman, "Static Fatigue of Optical Fibers in Bending II: Effect of Humidity and Proof Stress on Fatigue Lifetimes," Proc. SPIE 842, 32 (1987).

15. L. D. Merkle, N. Koumvakalis, and M. Bass, "Laser-Induced Bulk Damage in SiO_2 at 1.064, 0.532, and 0.355 μm," J. Appl. Phys. 55, 772 (1984).

DISCLAIMER